# A SHADOWGRAPH METHOD FOR OCEAN ACOUSTICS

B.J. Uscinski University of Washington, Applied Physics Laboratory
and Department of Electrical Engineering, Seattle, Washington, USA
and University of Cambridge, Department of Applied Mathematics
and Theoretical Physics, Cambridge, U.K.

## ABSTRACT

Progress in theory and numerical simulations made over the last 20 years has greatly increased our insight into the structure of sound intensity in a randomly scattering ocean. This new knowledge is not merely of academic interest. It has allowed us to devise simpler, more practical approaches to remote sensing experiments. One such technique, the Acoustic Shadowgraph Method is described here and a specific example of its application is given.

## 1. INTRODUCTION

The ability to monitor large areas of the ocean by remote sensing using acoustics is of great practical importance. Some of the direct methods such as Conductivity, Temperature, Depth (C.T.D.) probes, and large towed chains measuring temperature and salinity either give information about specific locations or can be expensive and difficult to carry out. Existing remote sensing methods that use sound, such as acoustic tomography, can monitor hundreds of square kilometers of ocean over long periods but are expensive to operate and interpret. This is because tomography relies on accurate measurements of phase, or travel time, and the acoustic data must then be processed by computers using some sort of inverse method to reveal the required ocean features. Accurate phase measurements involve expensive instrumentation and installations, and the computing needed for inversion can be quite intensive. On the other hand our knowledge of the structure of an acoustic field propagating in an ocean containing random structure has advanced considerably

over the last 20 years and it is now possible to devise new measurement techniques that do not rely on phase or travel times.

One such method uses acoustic intensity alone and is therefore relatively simple to implement. We shall call this approach the Acoustic Shadowgraph Method. In principle it is not new. The shadowgraph, which relies on measuring only intensity, has been used in other branches of experimental physics for many years. Both radiophysics and radioastronomy have used the patterns of varying intensity produced when a radio-star is viewed through the ionosphere or interplanetary medium in order to investigate both the structure of the media and their motions[1],[2]. The ocean presents a more difficult case since it involves heavier volume scattering, but our advances in scattering theory [3]–[8] allowed us to apply these existing techniques to the ocean. This paper gives a description of the Shadowgraph Method as applied to Ocean Acoustics and presents a specific case of its use.

## 2. SOME KEY FEATURES OF INTENSITY FLUCTUATIONS

In order to understand why the acoustic shadowgraph method is possible and how it works we need to sketch out briefly some of the more important features of the intensity fluctuations that arise in an acoustic wave when it propagates in a medium with a randomly varying sound speed. The first of these is the fact that the intensity fluctuations have a structure that is very elongated in the direction of propagation.

### 2.1 Sound Ribbons

Numerical simulations of the field from a point source propagating in a random medium have not only helped to confirm the correctness of analytical expressions for the variance of intensity fluctuations, but have also revealed important characteristics of their behaviour.[9] For example, in Fig. 1, which shows the result of a numerical simulation of propagation from a point source, the peaks in the trace correspond to regions of enhanced intensity. We note that such regions are very much elongated in the direction of propagation compared with the transverse scale. This fact is crucial in the shadowgraph method. Because of this elongation it is not necessary for the hydrophone to be towed on a precisely circular path. If intensity alone is recorded then small deviations from a circular track will have little effect on the fluctuation statistics at that general range. If the method were to rely on phase measurements then lateral motion of the hydrophone and deviations from a circular track would lead to large effects and such an experiment would not be practical. These elongated features or "sound ribbons" have not only been predicted by numerical simulations but evidence supporting their existence has come from a large scale ocean acoustic experiment.[10],[11]

### 2.2 Variance of the Intensity Fluctuations

The next point to consider is the strength of the intensity fluctuations. Physical

intuition tells us that the fluctuations will be weak for small distances of propagation but should increase with distance. The quantity most widely used to describe the strength of the intensity fluctuations is their normalised variance. If $I$ is the fluctuating acoustic intensity the normalised variance is defined as

$$\sigma_I^2 = (< I^2 > - < I >^2)/ < I >^2, \tag{1}$$

which is sometimes referred to as the "Scintillation Index". The behaviour of $\sigma_I^2$ is known from theory [6] and numerical simulations.[9] A typical set of curves for $\sigma_I^2$ is given in Fig. 2 as a function of $X$ the scale range. If $x$ is the unscaled coordinate in the direction of propagation, $k$ the wave number of the acoustic field and $L_m$ the scale size of the random irregularities in the medium then

$$X = x/kL_m^2. \tag{2}$$

The behaviour of $\sigma_I^2$ also depends on the strength of the scattering

$$\Gamma = k^3\mu^2 L_m^3 \tag{3}$$

where

$$\mu^2 = (\frac{\Delta C}{C})^2 > \tag{4}$$

is the mean fractional variation in sound speed $C$.

The precise shape of the $\sigma_I^2(X)$ curves depends, to some extent, on the specific type of random irregularities in the medium, i.e. the form of their spatial frequency spectrum. However, for many natural random media the scale size $L_m$ represents the largest structure present, i.e. it is an 'outer' scale size. In this case the general behaviour of $\sigma_I^2(X)$ remains fairly much the same (Fig. 2) exhibiting a rise $A$, a peak greater than unity $B$ for the larger values of scattering strength $\Gamma$, and $C$ a subsequent decline to a 'saturation' value.

The reason for such a 'saturation' level of $\sigma_I^2(X)$ is as follows. When the distance of propagation is much greater than $L_m$ the field is the result of scattering by many statistically independent layers of thickness of the order of $L_m$. This follows from the definition of $L_m$ as a 'correlation length'. Since each layer has a random content and the distance of propagation from most of the layers is large, the total scattered field is composed of many independent and randomly phased contributions from the various layers. This means that at very large distances the probability distribution of the field will tend to a two-dimensional Gaussian and the corresponding distribution of intensity will be exponential. Then $\sigma_I^2$, Eq. (1), will take a value of unity.

At this stage it should be noted that in cases where there is no definite 'outer' scale the above arguments do not hold. The field might not necessarily 'saturate' at large distance, or if it does its saturation value might not be unity. However, in the case

# A Shadowgraph Method for Ocean Acoustics - B.J. Uscinski

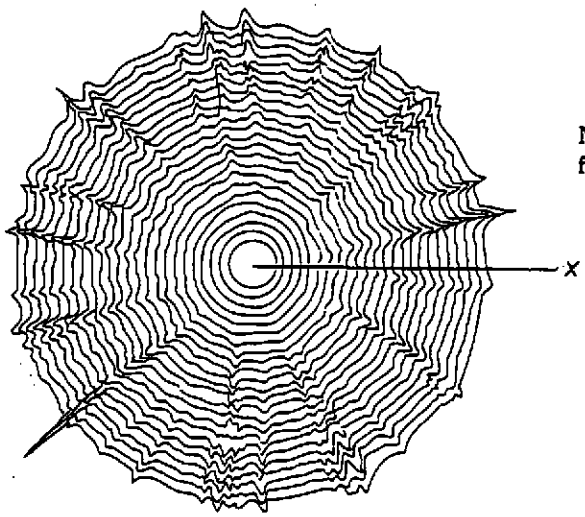


Fig. 1

Numerical simulation of acoustic intensity when the field from a point source propagates in a random medium.

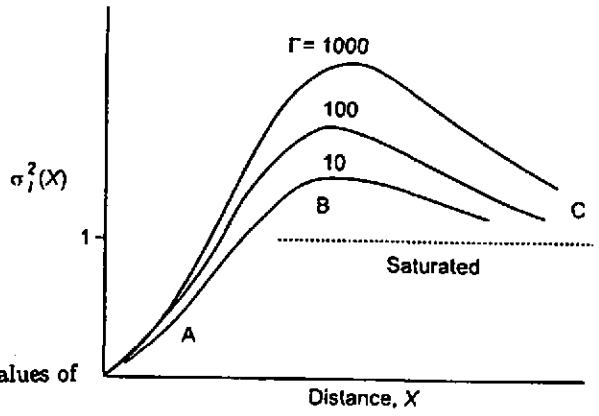


Fig. 2

A typical set of curves for $\sigma_I^2$ as a function of $X$ the scaled range. These are given for several values of $\Gamma$ the strength of scattering.

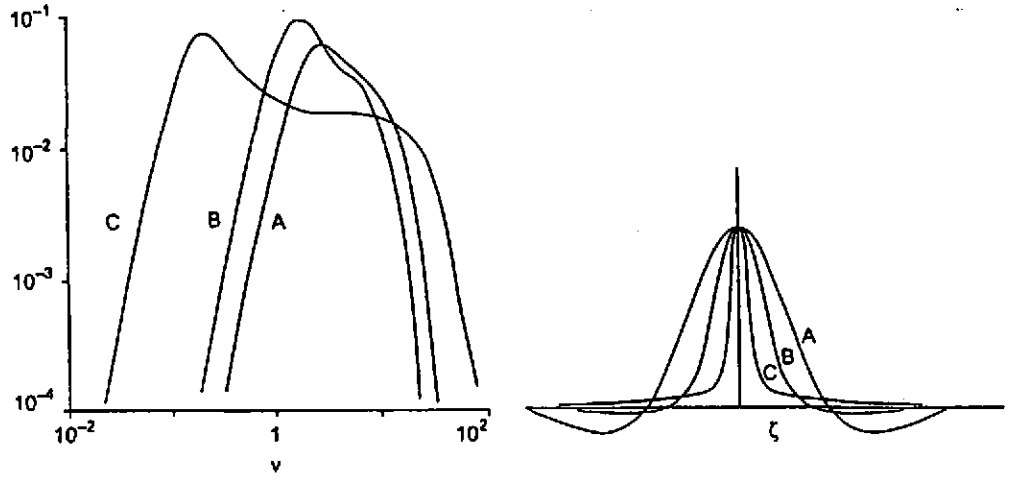


Fig. 3

Three typical spatial frequency spectra for positions A, B, and C on the $\sigma_I^2(X)$ curves of Fig. 4. Here $\nu$ is the spatial frequency scaled as explained in the text.

The spatial autocorrelation functions corresponding to the spectra of Fig. 5a. Here $\zeta$ is the spatial separation scaled by $L_v$.

of ocean sub-surface irregularities there appears to be a well defined 'outer'scale. This is also the case in very many natural random media.

For many situations where the shadowgraph method can be used the scintillation index will lie on the rising part of the curve. In this region a relationship of the following form is an excellent approximation

$$\sigma_I^2 = \alpha \Gamma X^\nu, \tag{5}$$

where $\alpha$ is a numerical constant usually of the order of 0.2 and $\nu$ is a power that generally lies between 2 and 3 for most natural irregular media. In the case of the ocean $\nu$ is close to 2.5 if internal waves or turbulent features predominate.

If the acoustic transmissions lead to an observed value of $\sigma_I^2 < 1$ then the experiment lies on the rising part of $A$ of the $\sigma_I^2(X)$ curve and useful information is directly available. If the observed $\sigma_I^2$ is larger than unity there could be some ambiguity in deciding just where it lies on the $\sigma_I^2(X)$ curve but there may be additional information that can help.

### 2.3 The Spatial Frequency Spectrum

If the shadowgraph trial is carried out by towing either the acoustic source or the receiving hydrophone then the observed fluctuating intensity pattern (the acoustic twinkling) gives the spatial structure of the sound field. Its spectrum will be the spatial frequency spectrum of the varying intensity, while the Fourier Transform of this gives the spatial autocorrelation function of the fluctuations. Three typical spectra are given in Fig. 3a for positions A, B, and C on the $\sigma_I^2(X)$ curves. The corresponding normalised autocorrelation functions appear in Fig. 3b. The spatial frequency $\nu$ in Fig. 3a is scaled so that $\nu = \nu_1 L_v$ where $\nu_1$ is the unscaled spatial frequency. In Fig. 3b $\zeta$ is the scaled spatial separation i.e. $\zeta = (z_1 - z_2)/L_v$.

The width of the normalised spatial autocorrelation function where it falls to a value of $e^{-1}$ gives the scale size of the intensity fluctuations $L_I$. This is related to $L_m$ the scale size of the random irregularities in the medium by the following approximate relationships. for a point source at position A

$$L_I \approx \sqrt{3} L_m \tag{6}$$

while at positions B and C

$$L_I \approx \sqrt{\frac{3}{\Gamma X}} L_m \tag{7}$$

Thus the autocorrelation function of the observed intensity fluctuations gives some fairly direct information about the spatial scale of the random structures in the medium.

## A Shadowgraph Method for Ocean Acoustics - B.J. Uscinski

### 2.4 Probability Distributions of Intensity

Another important descriptor of the fluctuating acoustic intensity is its probability distribution. This can be constructed from the observed intensity and compared with the distributions obtained from numerical simulations. Several simulated distributions calculated by Professor T.E. Ewart [12] are shown in Fig. 4 and are reproduced here with his kind permission. The gradual progression from something almost like a delta function at small ranges to a quasi-exponential form at very large ranges is clear. This allows the observed distribution to be placed in the appropriate position in the sequence without too much trouble, thus giving some confirmation as to the strength of scattering and range of propagation.

### 2.5 Pulse Broadening by Scatter

So far we have been concerned with the fluctuating intensity pattern observed when either the source or receiver moves. However, the acoustic transmissions will usually consist of a series of pulses so that the direct path between source and receiver can be isolated. The distortion of the individual pulses by scattering in the random medium also contains information and we now consider this.

For the sake of simplicity we shall take the transmitted pulse to have the form of a delta function in time. If there were no scattering by the medium then there would be only one path to the receiving hydrophone and the received pulse would also have the form of a delta function, Fig. 5a. The presence of irregular structures in the medium leads to scattering of the acoustic field and so there will be a number of random paths from source to receiver. The sound will take longer to traverse the various paths and will not all arrive simultaneously. In other words the pulse will be broadened or "smeared out" in time, Fig. 5b.

The subject of pulse broadening by scattering in a randomly irregular medium has been well studied and the general behaviour of the time-broadened pulse is shown in Fig 6 for different amounts of scatter. As is to be expected the greater the distance of propagation the more scattering and the greater the time spreading. For relatively large amounts of scatter $\Gamma X \geq 1$ the pulse spread is related to the scale size $L_m$, wave-number $k$, variation of sound speed $\mu^2$, and range $x$, but the overall form of the pulse spread tends to be independent of the spatial frequency spectrum of the medium. However, observations of pulse spread give an independent estimate of a combination of these quantities and so can be useful in conjunction with the other intensity quantities discussed above.

For smaller amounts of scatter $\Gamma X < 1$ there is a direct relationship between the pulse spread function and the spatial frequency spectrum of the random medium. Accurate determination of the pulse spread function could, in principle, give us the spatial frequency spectrum of the medium. In practice, however, this may not be possible since the spread times may be very small and the measurements lack the

# A Shadowgraph Method for Ocean Acoustics - B.J. Uscinski

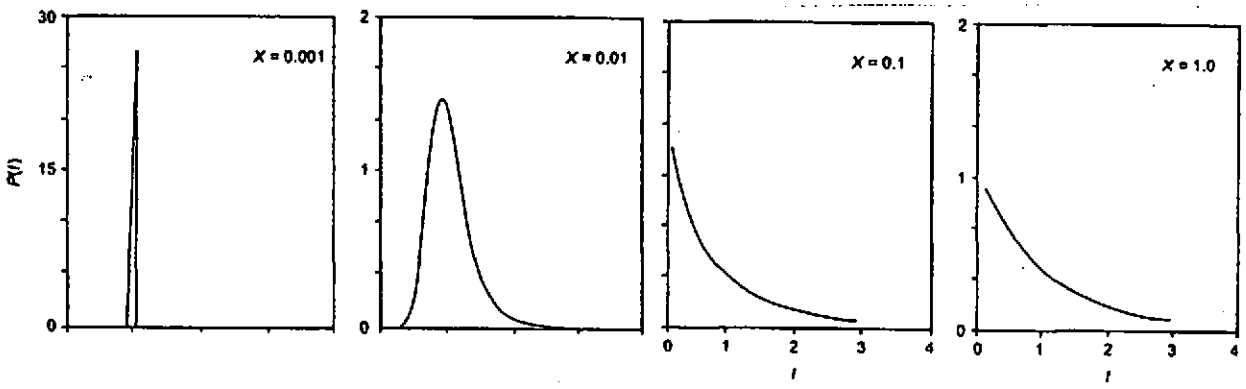


Fig. 4 Intensity probability distributions at increasing ranges in a multiply scattering medium as given by numerical simulations.

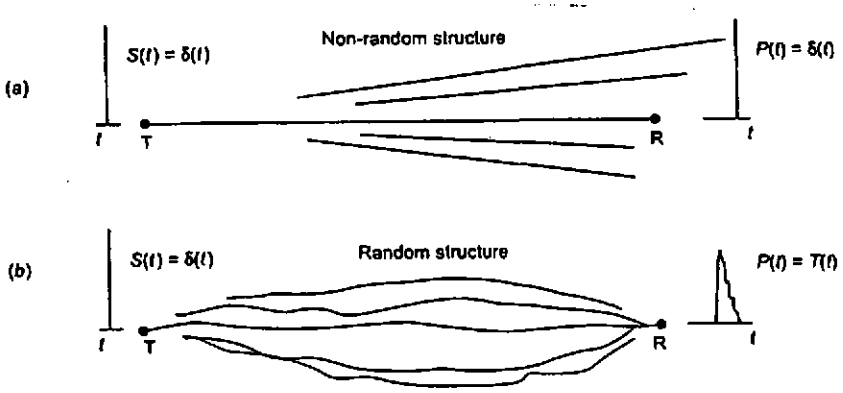


Fig. 5 (a) Ray paths and pulse shape in the absence of scattering.
(b) Ray paths and spread pulse in the presence of scattering.

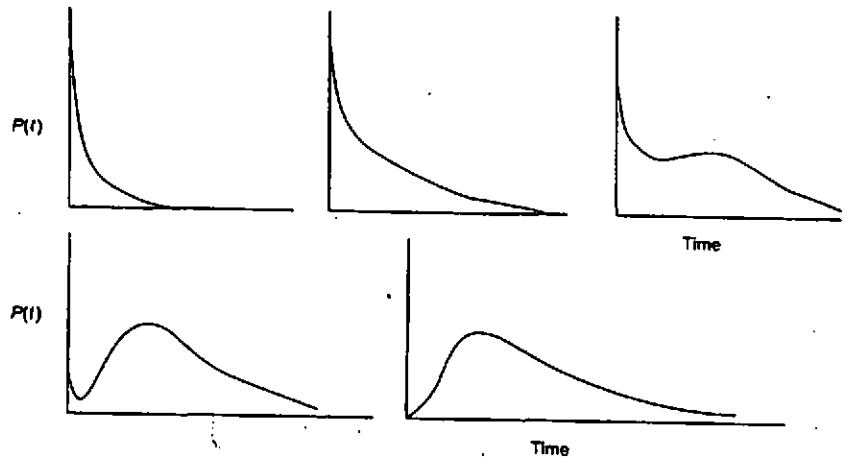


Fig. 6 Successive time broadening of a pulse with increasing amounts of scattering by a random medium.

necessary resolution. Nevertheless, these is one simple physical relationship that is important for such "singly-scattered" pulses. The time delay is related to the angle of scatter $\theta_s$ which in turn is related to the scale size of the medium and wavelength of the propagation field by

$$\theta_s \sim \lambda/\pi L_m \tag{8}$$

Thus the relatively large scale sizes will be responsible for the very small time delays corresponding to the sharp fall-off at the beginning of the broadened pulse (Fig. 6). There will be smaller features present and these, leading to larger scattering angles $\theta_s$ characterise the larger delay times at the tail of the broadened pulse. Also, if there is a cut-off time beyond which there is negligible pulse broadening then this cut-off will allow us to make an estimate of the smallest features that are present in appreciable quantities in the medium. This is an important additional piece of information that can not be obtained from observations of the fluctuating intensities alone.

## 3. PRINCIPAL FEATURES OF THE METHOD

It is important to remember that the Acoustic Shadowgraph method outlined above differs fundamentally from Acoustic Tomography, which is also used to map out internal features in the ocean. Tomography relies on accurate measurements of travel times as well as amplitudes. It can map larger regions of ocean than will probably be possible with the Shadowgraph Method, but the instrumentation it requires is much more complicated and expensive., On the other hand, the Shadowgraph approach records only intensities and does not need to measure phase or travel times. The equipment involved is much simpler and less expensive.

### 3.1 Specific Estimates

What can the Shadowgraph method tell us? Briefly, when used over ranges when $\sigma_I^2(X)$ lies on the rising part of the curve, it is possible to make a direct estimate of $L_m$ (Eq. 6). Since $k$ and $x$ are known we then have $X$ (Eq. 2) and $\Gamma$ (Eq. 5). This gives an estimate of $\mu^2$. Finally, analysis of the pulse time spread can give us an idea of the scale size of the smallest features present in appreciable quantities i.e. $L_{min}$. In summary we can hope to get estimates of $L_m, L_{min}$ and $\mu^2$.

### 3.2 The Wider Picture

If the irregular features in the medium differ in their diversity or strength in different sectors of the transmission this should also be evident from the observed intensity patterns. Some various cases are shown in Fig. 7 with different dispositions of the internal features and the corresponding intensity fluctuation pattern. It is fairly clear from the figure how the intensity pattern is related to the features and so a detailed explanation need not be given. The intensity shadowgraph method can give us an idea of the broader picture of how the features are distributed in the

# A Shadowgraph Method for Ocean Acoustics - B.J. Uscinski

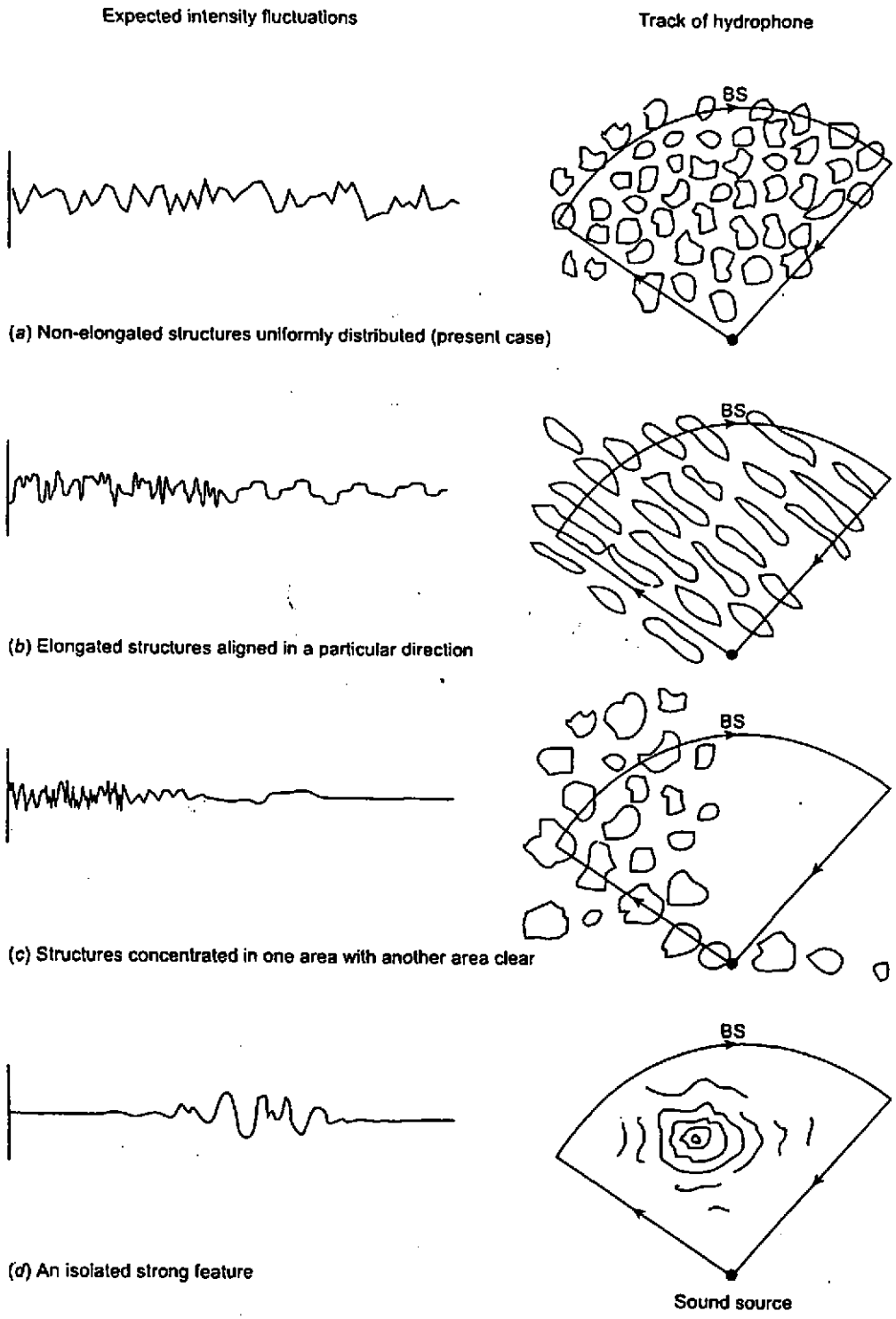


Fig. 7 Some different configurations of sub-surface structures and the expected appearance of the associated acoustic intensity fluctuations.

region under surveillance, as well as clues to whether they are isotropic in shape, elongated, uniform in size or not.

### 3.3 Merits and Drawbacks

The main merit of the Intensity Shadowgraph Method is its simplicity and robustness. It records intensity only and, because of the elongated nature of intensity fluctuations, the precision with which the hydrophone is located is not too important. The instrumentation involved is relatively simple and not too expensive. On the negative side, the ranges over which it can be used may be rather limited while the flow noise generated when towing the receiving hydrophones can pose a serious problem. This can be overcome by using a more powerful source or employing a receiving array rather than a single hydrophone.

## 4. A CONCRETE EXAMPLE OF THE SHADOWGRAPH METHOD. THE ACOUSTIC SEA-TRIAL OF 15.2.1997

We now describe an actual sea-trial in which the Acoustic Shadowgraph method was employed. It took place on 15th February, 1997 and was carried out from the Icelandic Research Vessel "Bjarni Saemundsson' at $60°N37'68'', 20°W42'03''$, (Fig. 8). The overall layout of the trial is shown in Fig. 9. The acoustic source suspended below a free floater (Fig. 10) carrying location equipment emitted sharp pulses at regular intervals. The research ship towed the receiving hydrophone set on a circular track at a suitable range from the source, and the received fluctuating acoustic signal was recorded on board. In the presence of irregular features in the upper ocean the acoustic intensity should look like the radial pattern shown in Fig. 1.

The ship's navigation system provided us with a G.P.S. plot of the position of the BS during the experiment (Fig. 11). The change in position of the floater between launch and recovery implies a drift of about 1.7 cm $sec^{-1}$ consistent with local currents. The water depth at the experimental location was about 350 m. The track of the ship relative to the floater is shown in Fig. 12 together with the current vector.

In the present case the sound rays are bent upwards towards the surface. One goes directly from source to receiver, one undergoes a single bounce, and other rays can have two or more bounces. The two main rays corresponding to the sound-speed profile are shown in Fig. 13. The lower direct path corresponds to the first arrival and the upper surface-reflected path to the second. The acoustic intensity (from pulse maximum value) is shown in Fig. 14 as a function of time.

## 5. RESULTS AND CONCLUSIONS

# A Shadowgraph Method for Ocean Acoustics - B.J. Uscinski

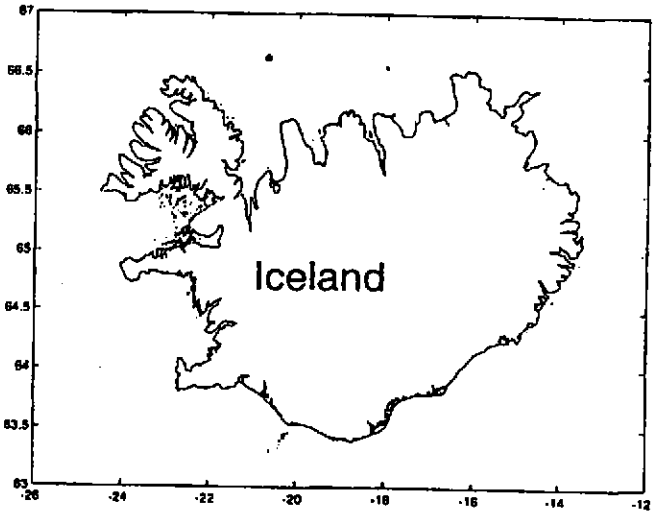


Fig. 8

Location of the shadowgraph experiment (heavy dot)

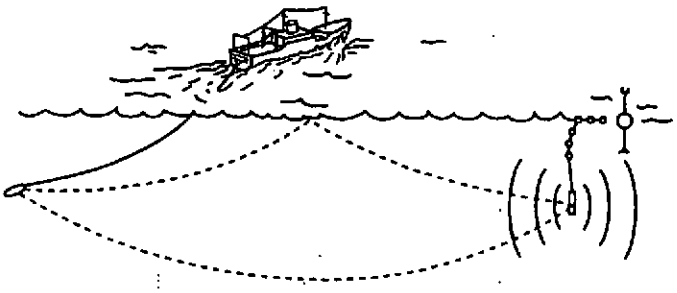

Fig. 9 General disposition of source, ship and hydrophones during acoustic shadowgraph transmissions.

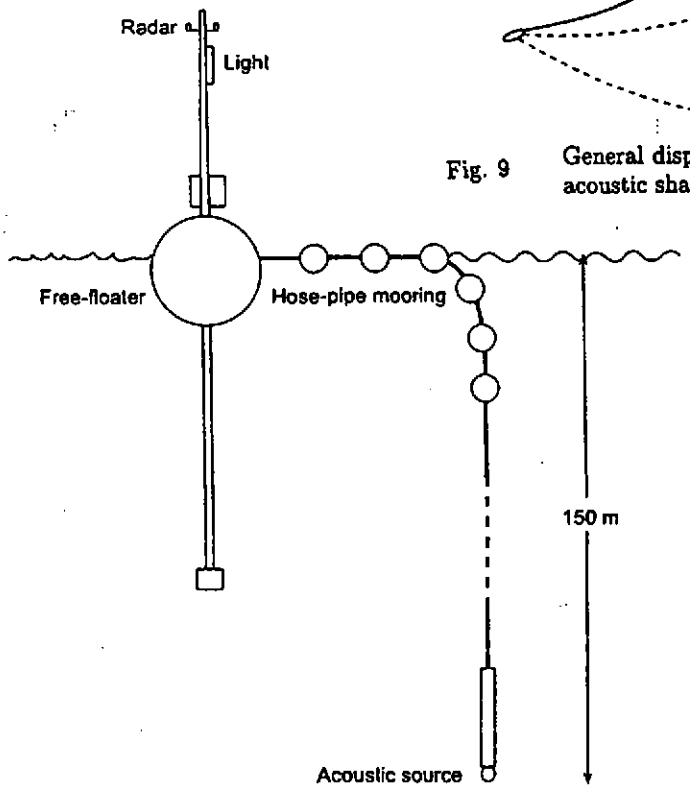


Fig. 10

The floater, hosepipe mooring and source.

## A Shadowgraph Method for Ocean Acoustics - B.J. Uscinski

### 5.1 Acoustic Intensity Fluctuations

The region that is of most immediate interest is the circular path, since at a constant range it is easiest to interpret the fluctuations in terms of propagation theory. For this reason an expanded and smoothed version of part of the intensity time series corresponding to the circular track is shown in Fig. 15. Smoothing by taking a running average over 10 consecutive pulses removes some of the high frequency fluctuations.

By inspecting Fig. 15 we see that there are major features in the fluctuating intensity of the order of 150 secs. At a steady steaming speed of about 1 m $\sec^{-1}$ these correspond to spatial variations of about 150 m.

The frequency distribution of the intensity is shown in Fig. 16. The circular track was subdivided into three equal sections and the distributions corresponding to the intensities of each section were calculated. These are superimposed in Fig. 16 and are seen to be quite consistent. This indicates that the statistics of the fluctuations along the circular track are fairly uniform. Comparison of this distribution with those obtained by numerical simulations and given in Fig. 4 shows a marked similarity with the $P(I)$ for $X \approx 0.01$. This agrees well with the value of $X$ derived for this trial on the basis of the observed scale size and given below in Eq. (12).

### 5.2 Normalized Variance or Scintillation Index

The first quantity to measure is the strength of the intensity fluctuations as characterized by their Normalized Variance or Scintillation Index, Eq.(1). The observed value in the present trial, as obtained from the intensity record on the circular path was

$$\sigma_I^2 \approx 0.15. \tag{9}$$

This tells us that it is region A on the rising part of the $\sigma_I^2(X)$ curves, Fig. 4, that is relevant to this trial.

### 5.3 Scale Sizes

The time fluctuations of intensity on the circular path, Fig. 15, are in fact spatial fluctuations through which the hydrophones are being towed. The speed of the ship is known and thus an estimate can be made of the spatial scale of intensity fluctuations transverse to the direction of acoustic propagation. This turns out to be

$$L_I \approx 150m. \tag{10}$$

Since $\sigma_I^2$ lies in region A of the propagation regime the intensity scale $L_I$ is related to that in the medium $L_m$ by Eq. (6), which implies a value of

$$L_m \approx 100m. \tag{11}$$

# A Shadowgraph Method for Ocean Acoustics - B.J. Uscinski

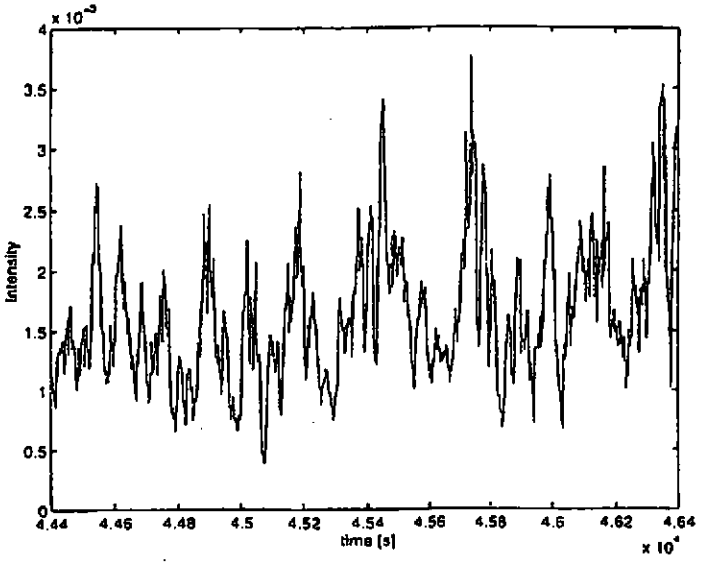


Fig. 15 Fluctuating acoustic intensity on part of the circular track. Very small scale features have been smoothed out.,

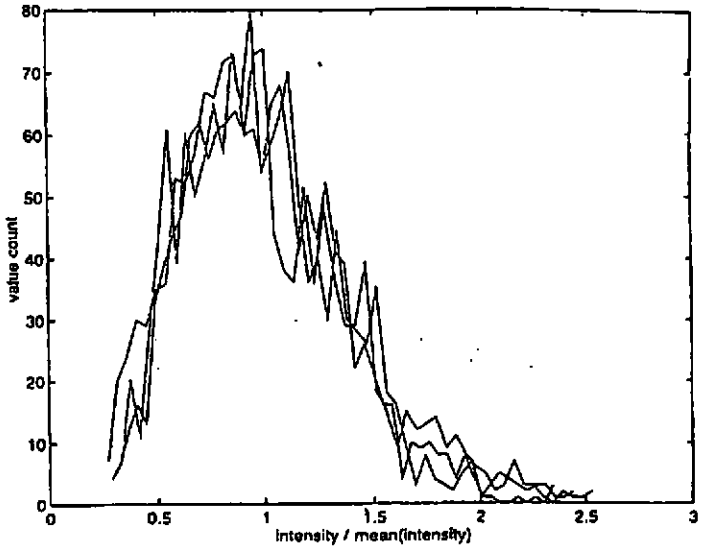


Fig. 16 Probability distribution of acoustic intensity from the smoothed time series on the circular track. The series was divided into three sections with a probability distribution for each section.

## A Shadowgraph Method for Ocean Acoustics - B.J. Uscinski

### 5.4 Scaled Range $X$

In the experiment the radius of the circular track $x$ was about 5.5 km, while for an acoustic frequency of 10 KHz the wave number $k \approx 40$. This implies a scaled range of

$$X = 1.37 \times 10^{-2} \tag{12}$$

### 5.5 The Scattering Strength $\Gamma$

In the region A where scattering is light to moderate $\sigma_I^2$ is given by Eq. (5) with $\nu \approx 2.5$ and $\alpha \approx 0.2$. Use of the values of $\sigma_I^2$ and $X$ given above yields

$$\Gamma \approx 3.4 \times 10^4, \tag{13}$$

and, further, in view of Eq. (3),

$$\mu^2 \approx 5.3 \times 10^{-7}. \tag{14}$$

### 5.6 Mean Fractional Variation in Sound Speed $\mu^2$

Independent estimates of $\mu^2$ can be made by analysis of the sound speed profiles obtained from the C.T.D. casts,, where irregular variations of the sound speed of the order of 1 m sec$^{-1}$ can be seen in the profiles taken at the stations closest to the trial, i.e. 62 and 63. The value of $\mu^2$ obtained from these profiles is

$$\mu^2 \approx 4.75 \times 10^{-7}, \tag{15}$$

which is close to that obtained by the shadowgraph method. It should also be remembered that the shadowgraph value is an average over a large area of ocean while that taken from the profiles corresponds to two particular places in that region.

### 5.7 Acoustic Pulse Broadening

Each pulse emitted by the source consisted of 50 cycles of the 10 KHz carrier wave and so was 5 m sec long. The pulse was repeated every two seconds. There were two paths from source to receiver Fig. 13, the direct path and that reflected from the sea surface. On both of these paths the pulse was broadened by scattering from the irregular features in the ocean, while the surface reflected pulse was additionally scattered by the surface waves. This scattering leads to distortion and time broadening of the received pulse. One such typical pulse is shown in Fig. 17. The main part is the direct pulse while the small tail is part of the surface scattered pulse. This surface scattered component arrived about 8 m sec after the direct pulse and so could be eliminated by time gating. In general the surface scattered pulse was very broken and indeed not always present. This was probably due to the fact the

the mean surface wave height was much greater than the 15 cm wavelength of the pulse carrier frequency, leading to very heavy scattering at the surface.

The direct pulse was much less distorted and a simple deconvolution enabled the time smearing effect of ocean scattering, sometimes called "the ocean transfer function", to be obtained.

### 5.8 Pulse Deconvolution

The average transfer function is shown in Fig. 18. We see that at small times $t \leq 0.05$ m sec the function $T(t)$ behaves like $t^{-2}$, while for $t > 0.05$ m sec it behaves more like the Gaussian function

$$\exp\{-t^2/t_0^2\}$$

where $t_0 \approx 0.01$ m sec. As mentioned above this time cut-off implies that there is a lower limit to the spatial scales present in the irregular structures. The simplest of physical considerations can give us an estimate of this smallest scale.

### 5.9 A Simple Physical Model

Let us assume that all the scattering medium is concentrated into a single layer halfway between the source and receiver Fig. 19. Although this may seem to be a gross simplification it has often been used to obtain practical estimates and it gives good results in practice. Simple geometry shows that the sideways displaced path is longer than the direct path by

$$\Delta x = \frac{x\theta_s^2}{2}. \tag{18}$$

The extra travel time involved is thus

$$\Delta t = x\lambda^2/2c\pi^2L^2 \tag{19}$$

where Eq. (8) for $\theta_s$ has been used. Expressing this in terms of the frequency $f$ we have

$$\Delta t = xc/2\pi^2L^2f^2 \tag{20}$$

#### 5.9.1 The Scale $L_m$

Analysis of the fluctuating intensity showed that the main spatial scale in the medium was of the order $L_m \approx 100$ m. If this is used in Eq. (20), together with the values $x = 5.5$ km, $c = 1500$ m sec$^{-1}$ and $f = 10$ KHz,m the resulting estimate for the time delay is

$$\Delta t \approx 0.04 \times 10^{-5}. \tag{21}$$

## A Shadowgraph Method for Ocean Acoustics - B.J. Uscinski

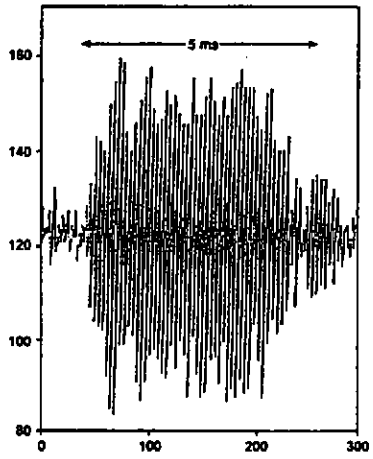


Fig. 17

A typical scattered pulse. The main part is that arriving by the direct path while the small tail is the surface scattered arrival.

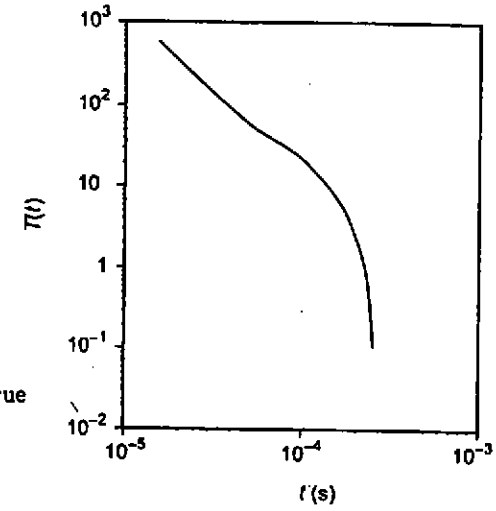


Fig. 18

The average transfer function. This would be obtained by averaging over many scattered pulses that were initially true delta or impulse functions.

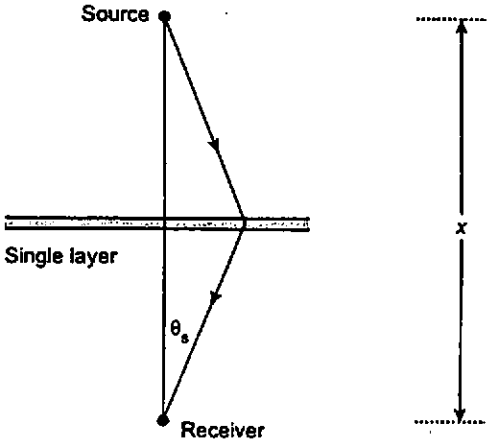


Fig. 19

Geometry of scattering with the medium compressed into a single layer halfway between source and receiver.

This is very small and lies below the time resolution achievable with the digitization interval used to process the acoustic data. If necessary a finer interval could be employed to resolve the pulse at very small times. However, it is the larger time delays that are of more interest since they contain information about the smaller features.

### 5.9.2 Smallest or "Inner" Scale $L_{\min}$

An estimate of the smallest scale present in appreciable quantity $L_{\min}$, can be obtained by setting the value of 0.01 m sec for $T_0$ in Eq. (20). This yields

$$L_{\min} \approx 6 \text{ to } 7 \text{ m.} \tag{22}$$

## 6. SUMMARY

Use of the shadowgraph method in the sea trial of 15.2.1997 gave us the following estimates for the irregular features present in the sub-surface layer at depths from about 150 to 200 m.

### 6.1 Fractional Variance of Sound Speed

$$\mu^2 = 5.3 \times 10^{-7}$$

which was in agreement with that obtained from C.T.D. measurements.

### 6.2 Outer $L_m$ and Inner $L_{\min}$ Scales

$$L_m \approx 100 \text{ m } L_{\min} \approx 6 \text{ to } 7\text{m.}$$

### 6.3 General Disposition of Features

The uniform characteristics of the intensity fluctuations over the circular path indicates that the irregular sub-surface features were uniformly distributed throughout the area surveyed by acoustic transmissions.

## A Shadowgraph Method for Ocean Acoustics - B.J. Uscinski

## REFERENCES

[1] Briggs B 1968 Correlation analysis for drifting patterns *J. Atmos. Terr. Phys.* **30** 1777-1789

[2] Lang K R and Rickett B J 1970 Nature **225** 528

[3] Shishov V I 1968 Theory of wave propagation in random media *Izv. Vyssh. Uchben. Zaved. Radiofir.* **11** 866-875

[4] Uscinski B J 1977 *The Elements of Wave Propagation in Random Media* (N.Y., London: McGraw-Hill)

[5] Ishimaru A 1978 *Wave Propagation and Scattering in Random Media Vol 2* (N.Y.: Academic) 412, 431

[6] Uscinski B J 1982 Intensity fluctuation in a multiply scattering medium Solution of the fourth-moment equation Proc. Roy. Soc. London Ser. A **380** 137-169

[7] Uscinski B J, Macaskill C and Spivak M 1986 path integrals for wave intensity fluctuations in random media *J. Sound Vibration* **106** 509-528

[8] Macaskill C and Ewart T E 1996 Numerical solution of the fourth-moment equation for acoustic intensity correlations and comparison with the mid-ocean acoustic transmission experiment *J. Acoust. Soc. Am.* **99** 1419-1429

[9] Uscinski B J 1989 Numerical simulations and moments of the field from a point source in a random medium *J. Mod. Opt.* **36** 1631-1643

[10] Uscinski B J and Potter J R 1988 Sound ribbons in the sea *Acoustics Bulletin* **13** No 4 24-28

[11] Potter J R, Uscinski B J and Akal T 1998 Random focussing of sound into spatially-coherent ribbons *Waves in Random Media* (submitted)

[12] Ewart T E 1989 A model of the intensity probability distribution for wave propagation in random media *J. Acoust. Soc. Am.* **86** 1490-1498.